Available online at www.sciencedirect.com
SCIENCE DIRECT®
Physics Letters B 633 (2006) 98–105
PHYSICS LETTERS B
www.elsevier.com/locate/physletb

Neutralino annihilation beyond leading order

Vernon Barger [a], Wai-Yee Keung [b], Heather E. Logan [a,c,*], Gabe Shaughnessy [a], Adam Tregre [a]

[a] *Department of Physics, University of Wisconsin, 1150 University Avenue, Madison, WI 53706, USA*
[b] *Physics Department, University of Illinois at Chicago, IL 60607-7059, USA*
[c] *Physics Department, Carleton University, Ottawa, Ontario K1S 5B6, Canada*

Received 31 October 2005; received in revised form 17 November 2005; accepted 18 November 2005

Available online 1 December 2005

Editor: M. Cvetič

Abstract

High-precision measurements of the relic dark matter density and the calculation of dark matter annihilation branching fractions in the sun or the galactic halo today motivate the computation of the neutralino annihilation cross section beyond leading order. We consider neutralino annihilation via squark exchange and parameterize the effective annihilation vertex as a dimension-six operator suppressed by two powers of the squark mass and related to the divergence of the axial vector current of the final-state quarks. Since the axial vector current is conserved at tree level in the limit of massless quarks, this dimension-six operator contains a suppression by the quark mass. The quark mass suppression can be lifted in two ways: (1) by corrections to the dimension-six operator involving the anomalous triangle diagram, and (2) by going to dimension-eight. We address the first of these possibilities by evaluating the anomalous triangle diagram, which contributes to neutralino annihilation to gluon pairs. We relate the triangle diagram via the anomaly equation to the decay of a pseudoscalar into two gluons and use the Adler–Bardeen theorem to extract the next-to-leading order (NLO) QCD corrections to $\chi\chi \to gg$ from the known corrections to pseudoscalar decay. The strong dependence of the dominant $\chi\chi \to q\bar{q}$ cross section on the relative velocity of the neutralinos makes these NLO corrections unimportant at χ decoupling but significant today.

1. Introduction

The presence of non-baryonic dark matter in the universe is compelling evidence for physics beyond the Standard Model. While many very different models have been proposed to explain the dark matter (wimps, axions, wimpzillas, modified gravity, etc.) [1], the thermal production of stable weakly-interacting particles with weak-scale mass remains as the most attractive and predictive explanation for the observed dark matter relic abundance, and further allows the solution to the dark matter problem to be linked to the solution to the hierarchy problem and tested at current and future collider experiments. Supersymmetry provides an especially attractive explanation with the lightest supersymmetric particle (LSP) as the dark matter candidate. Once such a weakly-interacting massive particle (χ) has been discovered and its couplings measured, it will be possible to compute its annihilation cross section (which controls its thermal relic abundance) and compare to the measured dark matter abundance to test our understanding of the microphysics of dark matter. The cosmological dark matter abundance is already measured at the 10% level to be [2]

$$\Omega_{\rm CDM}h^2 = 0.12 \pm 0.01 \quad (\text{SDSS} + \text{WMAP}),$$

and future cosmic microwave background experiments such as PLANCK expect to improve this to the few-percent level [3]. In order to match the expected few-percent precision of the cosmological measurements, we need both high-precision inputs from the colliders and high-precision calculations of the neutralino annihilation cross section. The latter requirement means going beyond leading order. High-precision calculations of the relic abundance are thus needed to match the microphysics onto cosmology.

* Corresponding author.
E-mail addresses: barger@pheno.physics.wisc.edu (V. Barger), logan@physics.carleton.ca (H.E. Logan), gshau@physics.wisc.edu (G. Shaughnessy), tregre@pheno.physics.wisc.edu (A. Tregre).

0370-2693 © 2005 Elsevier B.V. Open access under CC BY license.
doi:10.1016/j.physletb.2005.11.062

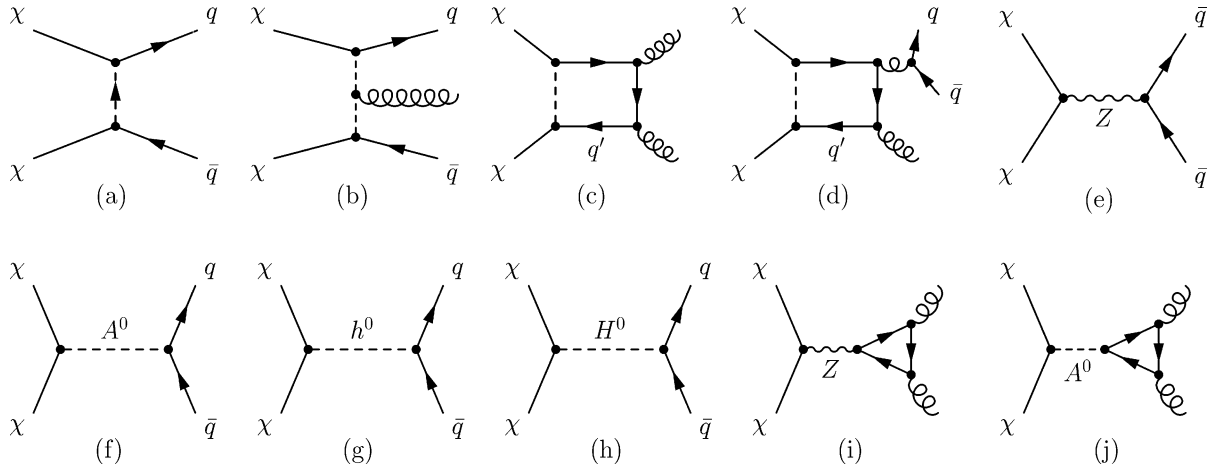

Fig. 1. Feynman diagrams that contribute to the total annihilation cross section: (a) the tree-level diagram, (b)–(d) t-channel squark exchange, and (e)–(j) s-channel Z and Higgs exchanges.

Another important physics application of these higher-order QCD corrections is the calculation of signals from WIMP annihilations in the galactic halo or in the interior of the Sun. The NLO corrections are potentially important in the evaluation of the branching fractions for the observable gamma ray and neutrino signals, respectively. As we shall see, these NLO corrections turn out to be much more important for the calculation of the observable gamma ray and neutrino signals than in the calculation of the relic density because of the strong dependence of the tree-level annihilation cross-section on the relative velocity of the neutralinos.

1.1. Neutralino annihilation cross section

The behavior of the annihilation cross section depends on the composition of the neutralino. Throughout this Letter we assume that the LSP is largely gaugino as motivated by mSUGRA models [4]. The processes that contribute to the cross section up to order α_s^2 and one loop are shown in Fig. 1. The tree-level diagram is shown in Fig. 1(a). Figs. 1(b)–(d) show the diagrams with t-channel squark exchange, whereas (e)–(j) show the diagrams with s-channel Z, H^0, h^0, A^0 exchanges. The gauge and Higgs bosons couple to the Higgsino part of the LSP and thus their contributions are suppressed for a mostly-gaugino neutralino.[1] The corresponding suppression factors for the s- and p-wave terms in the cross section are given in Table 1.

1.2. The anomaly equation

The leading contribution to neutralino annihilation via exchange of a squark of mass $\tilde{M}$, shown in Fig. 1(a), can be reduced to an effective vertex described by a dimension-six operator suppressed by $\tilde{M}^2$,

$$\mathcal{L} = \big(c/\tilde{M}^2\big)\mathcal{O}_6, \quad \mathcal{O}_6 = (\bar{\chi}\gamma_\mu\gamma_5\chi)\big(\bar{q}\gamma^\mu\gamma_5 q\big), \tag{1}$$

where c is a dimensionless coefficient. This dimension-six operator corresponds to taking the leading term in the expansion of the squark propagator in powers of $1/\tilde{M}^2$; in particular, we work in the limit $m_\chi^2 \ll \tilde{M}^2$.

In the static limit, where the relative velocity of the two neutralinos can be neglected, the operator $\mathcal{O}_6$ is related to the divergence of the axial vector current of the quarks $\bar{q}q$:

$$\mathcal{O}_6 \to \big[\bar{\chi}(i\gamma_5/2m_\chi)\chi\big]\big[\partial_\mu\big(\bar{q}\gamma^\mu\gamma_5 q\big)\big]. \tag{2}$$

In the massless quark limit, $m_q = 0$, the axial vector current is conserved at tree level, $\partial_\mu(\bar{q}\gamma^\mu\gamma_5 q) = 0$, and all tree amplitudes due to the dimension-six operator vanish; in particular, radiating additional gluons cannot lift the suppression. Even at the loop level, for example, diagrams involving the exchange of a virtual gluon, the suppression is still valid unless the anomalous triangle diagram is involved. This is the well-known partially-conserved axial current (PCAC) condition.

Indeed, only through the anomalous loop diagrams is the conservation of the axial vector current violated, in the form [8]

$$\partial_\mu\big(\bar{q}\gamma^\mu\gamma_5 q\big) = 2m_q\bar{q}i\gamma_5 q + \frac{\alpha_s}{4\pi}G^{(a)}_{\mu\nu}\tilde{G}^{(a)\mu\nu} \tag{3}$$

with $\frac{1}{2}\tilde{G}_{\mu\nu} = \epsilon_{\mu\nu\alpha\beta}G^{\alpha\beta}$ denoting the dual color field strength tensor. The simplest such anomalous diagram is shown in Fig. 1(c). Neglecting the mass of the internal quark q' and using the anomaly equation, this diagram can be written in the form

$$\mathcal{L}_{\text{eff}}(\chi\chi \to gg) = \left(\frac{c/m_\chi}{2\tilde{M}^2}\right)(\bar{\chi}i\gamma_5\chi)\frac{\alpha_s}{4\pi}G^{(a)}_{\mu\nu}\tilde{G}^{(a)\mu\nu}, \tag{4}$$

for $m_{q'} \ll m_\chi$. In the opposite limit, $m_{q'} \gg m_\chi$, the very heavy quark decouples; the top quark contribution can be neglected if $m_\chi \lesssim 100$ GeV. The leading-order (LO) calculation using the anomaly equation was first studied correctly by Ref. [7] in the $\gamma\gamma$ channel in QED.

The gluonic decay amplitude of a fundamental pseudoscalar, $A^0 \to gg$, is also related to the anomaly equation. This decay proceeds through a quark loop. In the heavy quark limit, $m_Q \gg m_A$, the divergence term on the left-hand side of Eq. (3)

[1] The Higgsino fraction suppression can be removed at the cost of going to one loop [5].

Table 1
Dependence of the cross section from each diagram on various suppression factors. The diagrams are shown in Fig. 1. The p-wave contribution to the cross section is shown only when it is important due to suppression or absence of the s-wave component. The column labeled "χ mixing" sketches the dependence of the cross section on the neutralino composition. Interference terms between the various diagrams carry a combination of the suppression factors corresponding to each diagram, and are not shown. We note that the Z-pole structure of diagram (i) is canceled by a numerator factor supplied in accordance with Yang's theorem [6,7].

Diagram	χ mixing	s-wave	p-wave
(a)	[Gaugino]^4	$[m_q/\tilde{M}^2]^2$	$v^2[m_\chi/\tilde{M}^2]^2$
(b)	[Gaugino]^4	$\alpha_s[m_q/\tilde{M}^2]^2+\alpha_s[m_\chi^3/\tilde{M}^4]^2$	
(c)	[Gaugino]^4	$\alpha_s^2[m_\chi/\tilde{M}^2]^2$	
(d)	[Gaugino]^4	$\alpha_s^3[m_\chi/\tilde{M}^2]^2$	
(e)	[Higgsino]^4	$[m_q/(s-m_Z^2)]^2$	
(f)	[Gaugino × Higgsino]^2	$[(m_q/m_W)m_\chi/(s-m_A^2)]^2$	
(g)	[Gaugino × Higgsino]^2	0	$v^2[(m_q/m_W)m_\chi/(s-m_h^2)]^2$
(h)	[Gaugino × Higgsino]^2	0	$v^2[(m_q/m_W)m_\chi/(s-m_H^2)]^2$
(i)	[Higgsino]^4	$\alpha_s^2[m_\chi/m_Z^2]^2$	
(j)	[Gaugino × Higgsino]^2	$\alpha_s^2[m_\chi/(s-m_A^2)]^2$	

becomes insignificant, leading to

$$0 \simeq 2m_Q\bar{Q}i\gamma_5 Q + \frac{\alpha_s}{4\pi}G^{(a)}_{\mu\nu}\tilde{G}^{(a)\mu\nu}. \tag{5}$$

Note that because the Yukawa coupling of A^0 to the quark Q is proportional to the quark mass, the m_Q dependence of the $A^0 \to gg$ partial width drops out in the limit $m_Q \gg m_A$.

In contrast, the neutralino pair annihilates into two gluons via the anomaly diagram, which is dominated by light quarks, $m_q \ll m_\chi$. In this limit, the term proportional to m_q on the right-hand side of Eq. (3) becomes insignificant, leading to

$$\partial_\mu\bar{q}\gamma^\mu\gamma_5 q \simeq 0 + \frac{\alpha_s}{4\pi}G^{(a)}_{\mu\nu}\tilde{G}^{(a)\mu\nu}. \tag{6}$$

Thus we see that two seemingly different processes, $A^0 \to gg$ through a heavy quark loop and $\chi\chi \to gg$ through a light quark loop, are related by the anomaly equation to the *same* gluonic operator. The Adler–Bardeen theorem [9] guarantees that the anomaly equation, Eq. (3), is valid to all orders of α_s. One can take advantage of this anomaly property to obtain the higher-order QCD corrections to $\chi\chi \to gg$ from the known results for $A^0 \to gg$ at next-to-leading order (NLO) from Ref. [10]. Note that, because of the non-Abelian nature of the gauge field, the above gluonic operator also incorporates tri-gluon amplitudes beyond leading order.

1.3. Beyond dimension-six

If we include higher terms in the $1/\tilde{M}^2$ expansion, the PCAC constraint will be lifted. The dimension-eight operator corresponding to an amplitude proportional to $1/\tilde{M}^4$ survives even in the massless quark limit, $m_q \to 0$. One can use this dimension-eight amplitude to calculate the rate of $\chi\chi \to q\bar{q}g$ from diagrams such as Fig. 1(b); a full calculation was done in Ref. [11]. However, the contribution to $\chi\chi \to q\bar{q}g$ from the dimension-six operator due to the anomaly with a virtual gluon turning into a quark pair (Fig. 1(c)) suffers less $\tilde{M}$ suppression and will dominate the dimension-eight term for $\tilde{M} \gg m_\chi$ even though the order in α_s is higher.

The effective vertex of the dimension-eight operator for $\chi\chi \to q\bar{q}g$ is

$$\mathcal{L} = \left(c_8 g_s^2/\tilde{M}^4\right)\mathcal{O}_8,$$
$$\mathcal{O}_8 = \epsilon_{\mu\nu\alpha\beta}G^{(c)\alpha\beta}\left(\bar{q}\gamma^\nu\gamma_5 t^c q\right)\left(\bar{\chi}\gamma^\mu\gamma_5\chi\right), \tag{7}$$

where $G^{(c)\alpha\beta}$ is the gluonic field strength for color index c and t^c is the corresponding SU(3) generator. This operator has exactly the same form as that in Eq. (6) of Ref. [12] for the $\chi\chi \to f\bar{f}\gamma$ amplitude computed through explicit expansion of the propagators to order $1/\tilde{M}^4$ in the limit $m_q = 0$.

It is interesting to note that the amplitude for $\chi\chi \to q\bar{q}g$ from the dimension-six operator with one gluon splitting into $q\bar{q}$ (shown in Fig. 1(d)) yields an operator of the same form as in Eq. (7). This allows the interference term between this diagram and the dimension-eight process to be easily obtained.

2. Calculation

2.1. The anomaly at leading order

Since neutralinos are Majorana in nature, the initial state behaves as a pseudoscalar in the zero-velocity limit [13]. In particular, for $v_{\rm rel} = 0$ the antisymmetrized neutralino spinors reduce to the projection operators [14]

$$u(p_1)\bar{v}(p_2) - u(p_2)\bar{v}(p_1)$$
$$= (m_\chi + \not{P})\gamma_5 = m_\chi\left(1+\gamma^0\right)\gamma_5, \tag{8}$$

where p_1 and p_2 are the four-momenta of the incoming neutralinos and $2P = p_1 + p_2$.

We work in the limit of zero fermion mass, in which case the off-diagonal terms in the squark mass matrices vanish and the squark mass eigenstates coincide with the electroweak eigenstates $\tilde{q}_L$ and $\tilde{q}_R$. Applying the reduction formula Eq. (8) to the amplitude of the $\chi\chi \to gg$ diagram shown in Fig. 1(d) allows us to write the amplitude for the diagram involving squark $\tilde{q}_i$ as

$$i\mathcal{M}_i = \frac{-\sqrt{2}g_s^2 g_{r/l}^2}{M^2_{\tilde{q}_{i,r/l}}} \times \int \frac{d^4q}{(2\pi)^4}\,\mathrm{Tr}\left[\mathcal{F}(q)_i^{\mu\nu,ab}\not{P}\gamma_5 P_{R/L}\right]\epsilon(k_1)^*_\mu\epsilon(k_2)^*_\nu, \tag{9}$$

where the neutralino–quark–squark couplings are defined for right- and left-handed squarks, respectively, as

$$g_r = -\sqrt{2}N_{11}g'Q,$$
$$g_l = -\sqrt{2}N_{11}g'(T_3 - Q) + \sqrt{2}T_3 N_{12}g. \tag{10}$$

Here T_3 is the squark isospin, Q is the squark electric charge, and N_{11} and N_{12} are the bino and wino components of the neutralino as defined in Ref. [15]. We also define $P_{R/L} = (1 \pm \gamma_5)/2$ in the usual way as the right- and left-handed projection operators. The external gluon momenta are called k_1 and k_2, and q is the momentum flowing in the loop.

The form factor $\mathcal{F}(q)_i^{\mu\nu,ab}$ for squark $\tilde{q}_i$ and the corresponding internal quark q_i is given explicitly by

$$\begin{aligned}\mathcal{F}(q)_i^{\mu\nu,ab} &= \frac{\not{q} - \not{k}_2 + m_{q_i}}{(q-k_2)^2 - m_{q_i}^2}\gamma^\nu t^b \frac{\not{q} + m_{q_i}}{q^2 - m_{q_i}^2}\gamma^\mu t^a \frac{\not{q} + \not{k}_1 + m_{q_i}}{(q+k_1)^2 - m_{q_i}^2} \\ &\quad + \frac{\not{q} - \not{k}_1 + m_{q_i}}{(q-k_1)^2 - m_{q_i}^2}\gamma^\mu t^a \frac{\not{q} + m_{q_i}}{q^2 - m_{q_i}^2}\gamma^\nu t^b \frac{\not{q} + \not{k}_2 + m_{q_i}}{(q+k_2)^2 - m_{q_i}^2}.\end{aligned} \tag{11}$$

The two terms in $\mathcal{F}(q)_i^{\mu\nu,ab}$ correspond to the two possible directions of fermion flow in Fig. 1(d). The diagrams with the neutralinos crossed are already included through the use of the antisymmetrized spinors in Eq. (8).

After summing over left and right squark states, the amplitude becomes

$$\begin{aligned}i\mathcal{M}_i = &-\int \frac{d^4q}{(2\pi)^4} 2\,\mathrm{Tr}\big[\mathcal{F}(q)_i^{\mu\nu,ab}\gamma^\alpha(V_i + A_i\gamma_5)\big] \\ &\times P_\alpha \epsilon(k_1)_\mu^* \epsilon(k_2)_\nu^*,\end{aligned} \tag{12}$$

with

$$V_i = \frac{\sqrt{2}g_s^2}{4}\left(\frac{g_r^2}{M_{\tilde{q}_{i,r}}^2} - \frac{g_l^2}{M_{\tilde{q}_{i,l}}^2}\right),$$
$$A_i = \frac{\sqrt{2}g_s^2}{4}\left(\frac{g_r^2}{M_{\tilde{q}_{i,r}}^2} + \frac{g_l^2}{M_{\tilde{q}_{i,l}}^2}\right), \tag{13}$$

with couplings $g_{r,l}$ given in Eq. (10).

After integrating Eq. (12), the piece involving the vector coupling vanishes due to the conservation of vectorial current (CVC): the contracted vector behaves as a divergence, so that the resulting vector coupling to multi-gluon states vanishes. Light quark masses can be neglected in the form factor if $m_b^2 \ll m_\chi^2$, and the top quark loop amplitude is suppressed if $m_\chi^2 \ll m_t^2$. In these limits, the loop amplitude sums over five massless quarks. Note that in the massless quark limit, the form factor $\mathcal{F}(q)_i^{\mu\nu,ab}$ becomes independent of the quark flavor i. The sum over quarks q_i in the loop can then be factorized into a sum over the coupling factors A_i times the universal massless form factor $\mathcal{F}(q)_i^{\mu\nu,ab}$.

The gluon production amplitude contains a pseudovector triangle diagram. This can be transformed to a pseudoscalar triangle diagram via the axial anomaly, Eq. (3), where $\partial_\mu = -2iP_\mu$. The anomaly is computed by relating it to the decay of a fundamental pseudoscalar Higgs boson A^0 to two gluons via a heavy quark loop. If the mass of the heavy quark Q is sufficiently large, $m_Q \gg m_{A^0}$, then from Eqs. (5) and (6) we have

$$2iP_\alpha \sum A_i \bar{q}_i \gamma^\alpha \gamma_5 q_i = 2m_Q \bar{Q} i\gamma_5 Q \sum A_i. \tag{14}$$

The amplitude becomes

$$\begin{aligned}i\mathcal{M} &= -2m_Q \sum A_i \int \frac{d^4q}{(2\pi)^4}\,\mathrm{Tr}\big[\mathcal{F}(q)_Q^{\mu\nu,ab}\gamma_5\big]\epsilon(k_1)_\mu^*\epsilon(k_2)_\nu^* \\ &= -\frac{m_Q^2}{\pi^2}\sum A_i C_0\big(0,0,s,m_Q^2,m_Q^2,m_Q^2\big)\,\mathrm{Tr}\big[t^a t^b\big] \\ &\quad \times \epsilon^{\mu\nu\alpha\beta}k_{1\alpha}k_{2\beta}\epsilon(k_1)_\mu^*\epsilon(k_2)_\nu^*,\end{aligned} \tag{15}$$

where $s = 4m_\chi^2$ and $C_0(0,0,s,m_Q^2,m_Q^2,m_Q^2)$ is a three-point Passarino–Veltman integral [16]. In the limit of heavy quark mass, $m_Q^2 \gg s$, the three-point integral reduces to $-1/2m_Q^2$. In this limit the dependence on the heavy quark mass drops out and the amplitude becomes

$$i\mathcal{M} = \frac{1}{2}\delta^{ab}\frac{\sum A_i}{2\pi^2}\epsilon^{\mu\nu\alpha\beta}k_{1\alpha}k_{2\beta}\epsilon(k_1)_\mu^*\epsilon(k_2)_\nu^*, \tag{16}$$

where we have used $\mathrm{Tr}[t^a t^b] = (1/2)\delta^{ab}$. Squaring the amplitude and integrating over phase space gives the leading-order ($\chi\chi \to gg$) annihilation cross section,

$$v_{\mathrm{rel}}\sigma_{\mathrm{LO}}(\chi\chi \to gg) = \frac{m_\chi^2}{64\pi^5}\left(\sum_{q_i} A_i\right)^2, \tag{17}$$

where in our approximation the sum runs over the five light quarks q_i. Our result agrees with that of, e.g., Ref. [11] in the limit $m_q = 0$.

2.2. Beyond leading order

As discussed in Section 1.2, we can use the Adler–Bardeen theorem [9] and Eqs. (5) and (6) to obtain the QCD corrections to the $\chi\chi \to gg$ annihilation cross section by exploiting the known results for pseudoscalar Higgs decays to gluon pairs, $A^0 \to gg$, beyond leading order.

The NLO QCD corrections to the $A^0 \to gg$ partial width were calculated by Spira et al. [10]. In the heavy top quark limit, for which our anomaly relation is valid, the NLO QCD corrections are given by a multiplicative factor [10], times the LO decay rate

$$\begin{aligned}&\Gamma_{\mathrm{NLO}}\big(A^0 \to gg\big) \\ &\quad = \Gamma_{\mathrm{LO}}\big(A^0 \to gg\big) \\ &\qquad \times\left[1 + \frac{\alpha_s}{\pi}\left(\frac{97}{4} - \frac{7}{6}N_f + \frac{33 - 2N_f}{6}\log\frac{\mu^2}{m_A^2}\right)\right],\end{aligned} \tag{18}$$

where μ is the renormalization scale. The integer N_f counts the number of quark flavors in the gluon splitting, with $N_f = 5$ for $m_b \ll m_\chi \ll m_t$. The diagrams that contribute to $A^0 \to gg$ at LO and NLO are shown in Fig. 2. The NLO final states include gg, ggg, and $g\bar{q}q$.

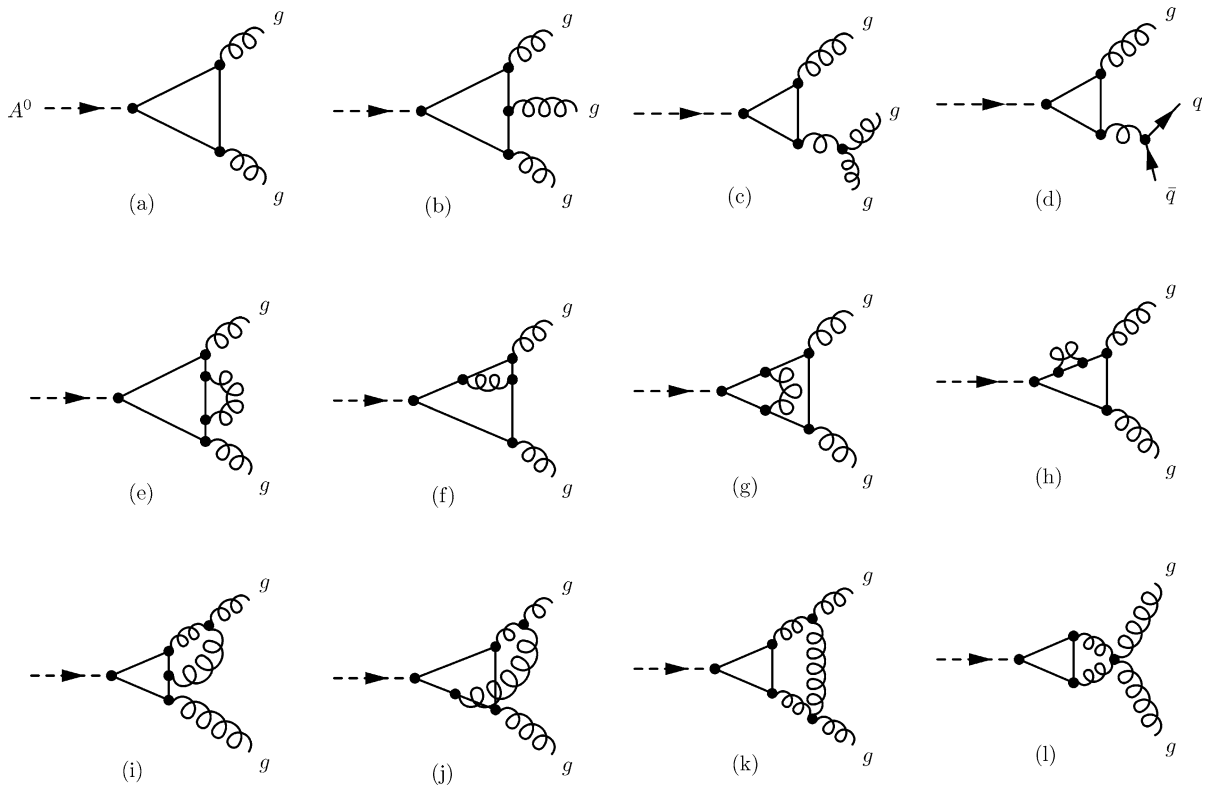

Fig. 2. LO and NLO diagrams for $A^0 \to gg$. (a) is the leading order process, (b)–(d) are the real emission diagrams with three final-state particles, and (e)–(l) are virtual corrections to diagram (a).

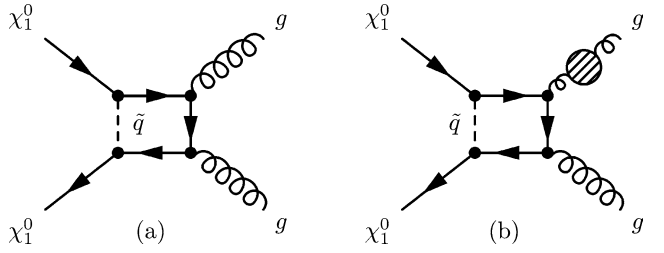

Fig. 3. $\chi\chi \to gg$ diagrams that supply a logarithmic factor to cancel that from Fig. 1(d). The one-loop corrections to the gluon legs include quark and gluon loops.

In $\chi\chi \to gg$ at NLO, a divergence occurs for the diagram in Fig. 1(d) when the final-state quarks are soft or collinear, in which case the gluon propagator diverges. This is the source of the logarithmic enhancement factor, $\log(m_\chi^2/m_q^2)$, found for this diagram in Ref. [12]. However, this logarithmic term is precisely canceled by the renormalization of the strong coupling due to the quark bubble that appears in the virtual part of the NLO correction, shown as the interference of the diagrams in Fig. 3. This is the familiar cancellation of logarithmic divergences guaranteed by the Kinoshita–Lee–Nauenberg theorem [17]. A similar cancellation occurs for the analogous diagrams in which the soft/collinear quarks are replaced with gluons.

We now invoke the Adler–Bardeen theorem [9] and take over the NLO corrections to $A^0 \to gg$ to the $\chi\chi \to gg$ process in the zero-velocity limit. In this correspondence, the pseudoscalar mass m_A is replaced by the $\chi\chi$ center-of-mass energy, equal to $2m_\chi$ in the zero-velocity limit. The NLO correction to the cross section for $\chi\chi \to gg$ follows immediately from Eqs. (17) and (18),

$$v_{\rm rel}\sigma_{\rm NLO}(\chi\chi \to gg) = \frac{m_\chi^2}{64\pi^5}\left(\sum A_i\right)^2 \times\left[1+\frac{\alpha_s}{\pi}\left(\frac{97}{4}-\frac{7}{6}N_f+\frac{33-2N_f}{6}\log\frac{\mu^2}{4m_\chi^2}\right)\right]. \quad (19)$$

We give explicitly the result for $\mu = 2m_\chi$ and $N_f = 5$,

$$v_{\rm rel}\sigma_{\rm NLO}(\chi\chi \to gg) = \frac{m_\chi^2}{64\pi^5}\left(\sum A_i\right)^2 (1+0.62), \quad (20)$$

where we set $m_\chi = 100$ GeV. The strong coupling is evaluated based on five-flavor running at the scale $\mu = 2m_\chi$ where it appears both explicitly and within the coefficient A_i. We note that the above choice of $m_\chi = 100$ GeV is well above the current experimental limit [18].

3. Numerical results

In this section we examine the validity of our assumption of massless quarks in the loop for the LO $\chi\chi \to gg$ calculation, show the improvement in the renormalization scale dependence obtained in going to NLO, and compare the $\chi\chi \to gg$ annihilation cross section to that of the leading-order tree-level process $\chi\chi \to q\bar{q}$ through t-channel squark exchange.

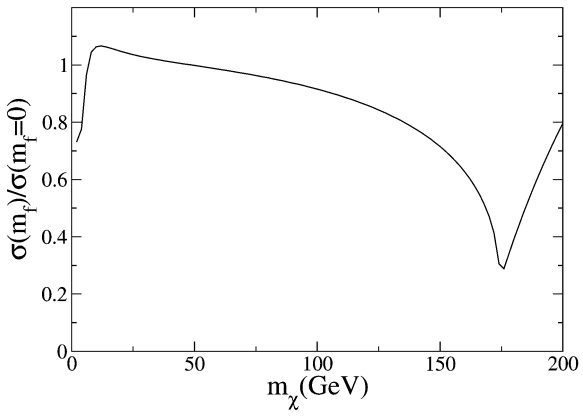

Fig. 4. The effect of quark masses on $v_{\rm rel}\sigma_{\rm LO}(\chi\chi \to gg)$. Shown is the full cross section including the quark mass dependence, normalized to the approximate cross section obtained by setting $m_q = 0$ for the five light quarks and $m_t = \infty$, for a common squark mass $\tilde{M} = 200$ GeV and a pure bino neutralino, $N_{11} = 1$, $N_{1j} = 0$ $(j \neq 1)$.

We have assumed in our use of the anomaly equation that the five light quarks running in the loop for $\chi\chi \to gg$ were massless, and we neglected the heavy top quark contribution. In Fig. 4, we test this assumption for the LO cross section by comparing our approximation to the full cross section including the quark mass dependence (we continue to use the $1/\tilde{M}^2$ approximation for the squark propagator). We plot the full cross section normalized to our five-massless-quark approximation as a function of m_χ. The full formula differs from our approximation by less than 10% for 6 GeV $< m_\chi <$ 110 GeV. For heavier neutralinos, the top quark loop starts to have a significant effect, with destructive interference occurring between the top loop and the lighter quark loops. Two of the top quarks in the loop go on shell at $m_\chi = m_t$, leading to the large dip in the cross section. For neutralinos lighter than about 6 GeV, the nonzero mass of the bottom quark begins to play a significant role, leading to the dip at lower masses.

In an all-orders calculation, physical observables cannot depend on the renormalization scale μ. The μ dependence of our predictions is an artifact of computing to a finite order in perturbation theory. The μ dependence can then be used to estimate the size of the uncomputed higher-order corrections. The dependence of the $\chi\chi \to gg$ annihilation cross section on the renormalization scale at LO and NLO is shown in Fig. 5(a) for $\tilde{M} = 200$ GeV, $m_\chi = 100$ GeV, and a pure bino neutralino, $N_{11} = 1$, $N_{1j} = 0$ $(j \neq 1)$.[2]

Varying μ by a factor of two in either direction from the central value $\mu = 2m_\chi$ yields a scale dependence of $\pm 16\%$ at LO and $\pm 9\%$ at NLO. The corresponding annihilation cross sections including scale uncertainty are shown in Fig. 5(b) as a function of m_χ.

Exact cross section formulae for all tree-level two-to-two neutralino annihilation processes are given in Ref. [19]. Using the expansion of the thermally averaged cross section in terms of $x = T/m_\chi$,

$$\langle v_{\rm rel}\sigma\rangle = a + bx, \tag{21}$$

one can compare the leading tree-level process, $\chi\chi \to q\bar{q}$ via t-channel squark exchange, to our results for $\chi\chi \to gg$ at NLO given in Eq. (20) both for annihilation during freeze-out in the early universe, $x \sim 1/20$, and for annihilation in the galactic halo today, $x \sim 0$ (corresponding to $v/c \sim 10^{-3}$). The cross sections for the two annihilation processes are shown in Fig. 6(a) as a function of m_χ for $\tilde{M} = 200$ GeV and a pure bino neutralino, with $x = 1/20$ and $x = 0$. For $\chi\chi \to q\bar{q}$ we sum the cross section over the five light final-state quark flavors and neglect $\chi\chi$ annihilation into lepton pairs. We use the running quark mass $m_q(\mu)$, which serves to resum the leading logarithmic QCD corrections to this process from soft gluon radiation [11], and take the renormalization scale $\mu = 2m_\chi$. The annihilation cross section for $\chi\chi \to gg$ is dominated by the s-channel component, and so we show only one curve for $x = 1/20$ and $x = 0$. The tree-level cross section for $\chi\chi \to q\bar{q}$ depends strongly on the relative velocity of the neutralinos, because the s-channel cross section is suppressed by the final-state quark mass. Thus the annihilation cross section at $x = 0$, which comes only from the s-wave component, is quite small and is comparable to that from $\chi\chi \to gg$. At $x = 1/20$, on the other hand, the $\chi\chi \to q\bar{q}$ cross section is dominated by the p-wave component and is larger than $\chi\chi \to gg$ by almost a factor of 100.

In Fig. 6(b) we show the corresponding K-factors, defined as the ratio of the total cross section, $\chi\chi \to q\bar{q} + gg$, to the tree-level $\chi\chi \to q\bar{q}$ cross section. This gives a measure of the relative importance of the $\chi\chi \to gg$ component of the total annihilation cross section. We see that during freeze-out, $x \sim 1/20$, the $\chi\chi \to gg$ contribution is quite small and $K = 1.01$–1.02 over the range of m_χ considered. In the present epoch, however, with $x \sim 0$, the K-factor is considerably larger, $K = 1.3$–30 depending on the mass of the neutralino. Such a large K-factor will impact annihilation branching fractions today, changing the gamma ray flux from the galactic halo and the neutrino flux from inside the Sun [1,11]. We note also that because both the $\chi\chi \to q\bar{q}$ and $\chi\chi \to gg$ annihilation cross sections have the same leading $1/\tilde{M}^4$ dependence on the squark mass, these K-factors will not depend significantly on the common squark mass scale.

We now exhibit the dependence of the annihilation cross section on the neutralino composition. Because we have worked in the zero-quark-mass limit in our calculation of $\chi\chi \to gg$, we have neglected the couplings of Higgsinos to the internal quark loop, which are proportional to the quark mass. We thus consider only mixed bino–wino neutralinos. We can then parameterize the mixing coefficients N_{1j} in terms of a bino–wino

[2] We note here that the renormalization scale dependence of the tree-level $\chi\chi \to q\bar{q}$ cross section arises only from the running quark mass in the s-wave contribution [11]. Since the cross section for this process is dominated by the quark-mass-independent p-wave part during freeze-out in the early universe, the scale dependence is negligible at tree level.

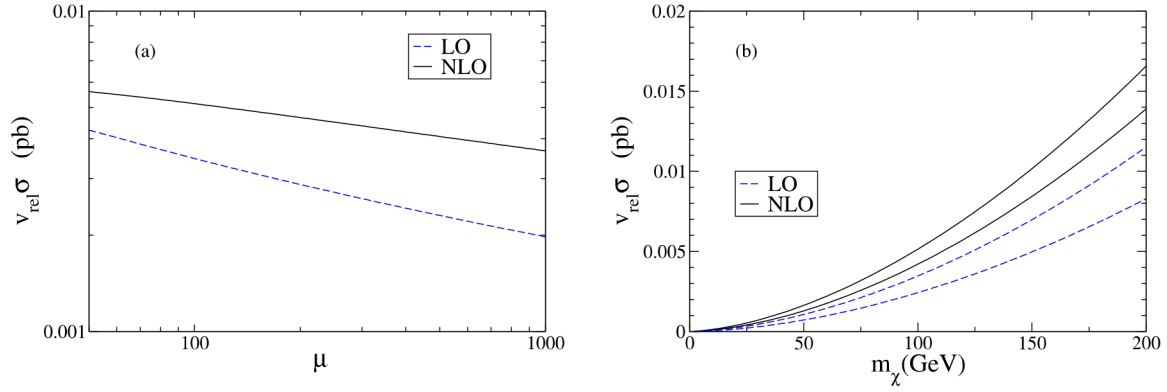

Fig. 5. Cross section for $\chi\chi \to gg$ at LO and NLO for a pure bino neutralino with $\tilde{M} = 200$ GeV. (a) Dependence on the renormalization scale μ for $m_\chi = 100$ GeV. (b) Dependence on m_χ showing the renormalization scale dependence in the band $\mu = m_\chi, 4m_\chi$.

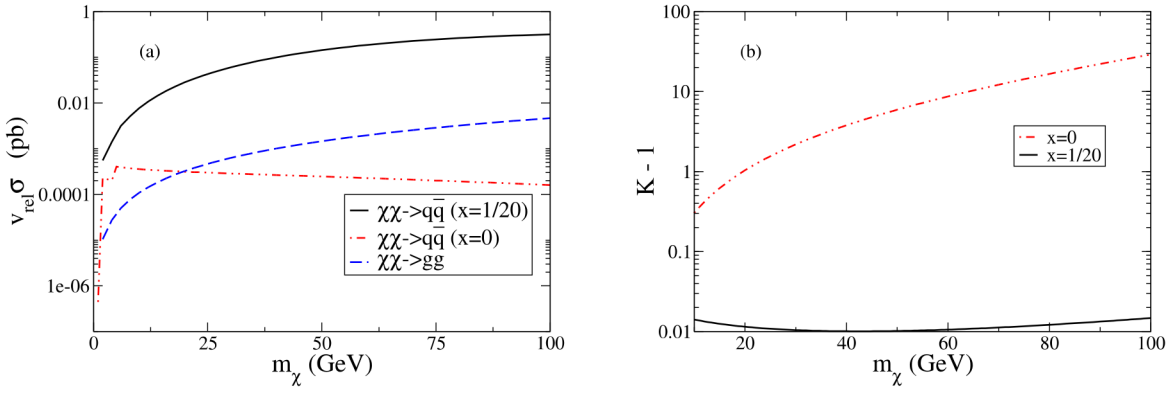

Fig. 6. (a) Annihilation cross sections for $\chi\chi \to q\bar{q}$ through t-channel squark exchange (diagram 1(a)) and $\chi\chi \to gg$ at NLO for $\tilde{M} = 200$ GeV and a pure bino neutralino. We show $\chi\chi \to q\bar{q}$ for both $x = 1/20$, corresponding to freeze-out in the early universe, and $x = 0$, corresponding to annihilation in the galactic halo at the present time. The steps in the $\chi\chi \to q\bar{q}$ cross section for $x = 0$ at low m_χ are due to quark mass thresholds. (b) Corresponding K-factors. We plot $K - 1$, which is the ratio of annihilation cross sections of $\chi\chi \to gg$ to $\chi\chi \to q\bar{q}$, for $x = 0$ and $x = 1/20$ as shown in (a).

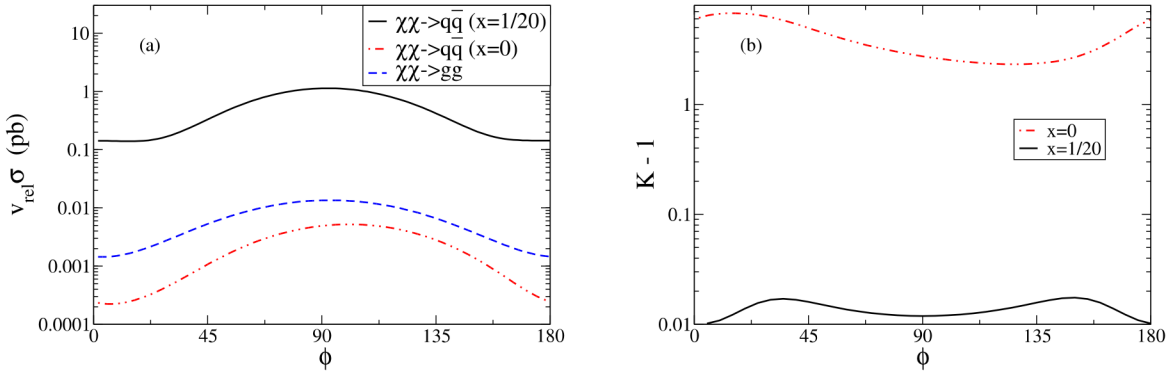

Fig. 7. (a) Annihilation cross sections for $\chi\chi \to q\bar{q}$ and $\chi\chi \to gg$ as in Fig. 6 as a function of the bino–wino mixing angle ϕ, for $m_\chi = 50$ GeV. Pure bino corresponds to $\phi = 0°, 180°$, and pure wino to $\phi = 90°$. (b) Corresponding K-factors.

mixing angle ϕ as

$$N_{11} = \cos\phi, \qquad N_{12} = \sin\phi, \qquad N_{13} = N_{14} = 0. \tag{22}$$

In Fig. 7 we again compare the leading tree-level process, $\chi\chi \to q\bar{q}$ via t-channel squark exchange, to our results for $\chi\chi \to gg$ at NLO. The cross sections for the two annihilation processes are shown in Fig. 7(a) as a function of the bino–wino mixing angle ϕ for $m_\chi = 50$ GeV, and $\tilde{M} = 200$ GeV, with $x = 1/20$ and $x = 0$. Again we take the renormalization scale $\mu = 2m_\chi$. There is a large enhancement of both annihilation cross sections if the neutralino has a large wino component, $\phi \sim 90°$, due to the stronger coupling of the wino to a quark–squark pair. In Fig. 7(b) we show the corresponding K-factors. The nontrivial dependence of the K-factors on ϕ arises from the interference among the five light quark loop diagrams that contribute to $\chi\chi \to gg$. By contrast, there is no interference between the amplitudes for $\chi\chi \to q\bar{q}$ with different flavor squarks in the t-channel be-

cause the internal squark flavor is fixed by the external quark flavor.

Finally, we note that the next-to-next-to-leading order (NNLO) corrections to $A^0 \to gg$ have been computed in Ref. [20]. One may be tempted to take this correction over to $\chi\chi \to gg$ in the same way as the NLO correction. However, at NNLO the $A^0 \to gg$ decay receives a contribution from the interference between the $G^{(a)}_{\mu\nu}\tilde{G}^{(a)\mu\nu}$ operator and a $\partial_\mu \bar{q}\gamma^\mu\gamma_5 q$ operator generated at two-loop level. Once effective operators other than $G^{(a)}_{\mu\nu}\tilde{G}^{(a)\mu\nu}$ appear, our use of the anomaly equation no longer applies. A proper treatment of $\chi\chi \to gg$ at NNLO would thus require a new calculation of the operator matching conditions and renormalization.

4. Conclusions

We reviewed the dependence of the main neutralino annihilation processes on various suppression factors—the Higgsino fraction, the quark and squark masses, and the relative neutralino velocity—and identified the dominant $\chi\chi \to q\bar{q}$ annihilation process for a gaugino-like neutralino as due to a dimension-six operator in the zero-velocity limit. This dimension-six operator contains the divergence of the axial vector current of the quarks $q\bar{q}$, which leads to the well-known quark mass suppression of the annihilation cross section. This quark mass suppression can be lifted in two ways: either through corrections to the dimension-six operator involving the anomalous triangle diagram, or by going to dimension-eight. We focused on the anomalous triangle diagram, which describes neutralino annihilation to gluon pairs. In the approximation of massless quarks running in the loop, the anomaly equation relates $\chi\chi \to gg$ to the seemingly unrelated process of pseudoscalar decay to gluon pairs via a very heavy quark loop. We used this relation to compute $\chi\chi \to gg$ in terms of the decay process $A^0 \to gg$. Further, taking advantage of the Adler–Bardeen theorem which guarantees that the anomaly equation is valid to all orders in α_s, we extracted the NLO QCD corrections to $\chi\chi \to gg$ from the known corresponding results for $A^0 \to gg$ and wrote them as a simple multiplicative factor that can be easily inserted into numerical neutralino annihilation codes. For $m_\chi = 100$ GeV and $\mu = 2m_\chi$, the NLO QCD corrections increase the annihilation cross section to gg by 62%. The NLO corrections also reduce the residual renormalization scale dependence of the $\chi\chi \to gg$ annihilation cross section from $\pm 16\%$ to $\pm 9\%$.

Our NLO results were computed in the approximation $m_b \ll m_\chi \ll m_t$. This approximation yields a LO $\chi\chi \to gg$ cross section within 10% of the exact result for $6\ \text{GeV} < m_\chi < 110\ \text{GeV}$. We finally compared our results for $\chi\chi \to gg$ at NLO to the dominant $\chi\chi \to q\bar{q}$ cross section in this neutralino mass range. For neutralino annihilation during freeze-out in the early universe, our results for $\chi\chi \to gg$ at NLO constitute only 1–2% of the dominant cross section for a gaugino-like neutralino and are thus of little importance for computing the relic neutralino abundance. However, for neutralino annihilation at the present time the relative neutralino velocity is much lower, leading to a much smaller tree-level $\chi\chi \to q\bar{q}$ cross section. In this situation, the $\chi\chi \to gg$ cross section can be as large or larger than $\chi\chi \to q\bar{q}$, so that NLO corrections can have a significant impact on the computation of gamma ray and neutrino fluxes from neutralino annihilation in the galactic halo and inside the Sun, respectively.

Acknowledgements

This work was supported in part by the US Department of Energy under grants DE-FG02-95ER40896 and DE-FG05-84ER40173 and in part by the Wisconsin Alumni Research Foundation. We thank W. Bardeen and M. Drees for helpful comments. V.B. thanks the Aspen Center for Physics for hospitality during the completion of this work.

References

[1] G. Bertone, D. Hooper, J. Silk, Phys. Rep. 405 (2005) 279, hep-ph/0404175.
[2] C.L. Bennett, et al., WMAP Collaboration, Astrophys. J. Suppl. 148 (2003) 1, astro-ph/0302207;
D.N. Spergel, et al., WMAP Collaboration, Astrophys. J. Suppl. 148 (2003) 175, astro-ph/0302209;
M. Tegmark, et al., SDSS Collaboration, Phys. Rev. D 69 (2004) 103501, astro-ph/0310723.
[3] J.A. Tauber, The PLANCK mission, in: M. Harwit (Ed.), IAU Symposium, Manchester, UK, 15–18 August, 2000, p. 493.
[4] S. Abel, et al., SUGRA Working Group Collaboration, hep-ph/0003154.
[5] A. Djouadi, M. Drees, P. Fileviez Perez, M. Muhlleitner, Phys. Rev. D 65 (2002) 075016, hep-ph/0109283.
[6] C.N. Yang, Phys. Rev. 77 (1950) 242.
[7] S. Rudaz, Phys. Rev. D 39 (1989) 3549;
L. Bergstrom, Phys. Lett. B 225 (1989) 372.
[8] S.L. Adler, Perturbation theory anomalies, in: S. Deser, M. Grisaru, H. Pendleton (Eds.), Lectures on Elementary Particles and Quantum Field Theory, vol. 1, MIT Press, Cambridge, MA, 1970, pp. 3–164.
[9] S.L. Adler, W.A. Bardeen, Phys. Rev. 182 (1969) 1517.
[10] M. Spira, A. Djouadi, D. Graudenz, P.M. Zerwas, Nucl. Phys. B 453 (1995) 17, hep-ph/9504378.
[11] M. Drees, G. Jungman, M. Kamionkowski, M.M. Nojiri, Phys. Rev. D 49 (1994) 636, hep-ph/9306325.
[12] R. Flores, K.A. Olive, S. Rudaz, Phys. Lett. B 232 (1989) 377.
[13] L. Bergstrom, H. Snellman, Phys. Rev. D 37 (1988) 3737.
[14] J.H. Kuhn, J. Kaplan, E.G.O. Safiani, Nucl. Phys. B 157 (1979) 125.
[15] P. Gondolo, J. Edsjo, P. Ullio, L. Bergstrom, M. Schelke, E.A. Baltz, JCAP 0407 (2004) 008, astro-ph/0406204.
[16] G. Passarino, M.J.G. Veltman, Nucl. Phys. B 160 (1979) 151.
[17] T. Kinoshita, J. Math. Phys. 3 (1962) 650;
T.D. Lee, M. Nauenberg, Phys. Rev. 133 (1964) B1549.
[18] S. Eidelman, et al., Particle Data Group, Phys. Lett. B 592 (2004) 1.
[19] T. Nihei, L. Roszkowski, R. Ruiz de Austri, JHEP 0203 (2002) 031, hep-ph/0202009.
[20] K.G. Chetyrkin, B.A. Kniehl, M. Steinhauser, W.A. Bardeen, Nucl. Phys. B 535 (1998) 3, hep-ph/9807241.